Neural Processing Letters (2024) 56:174
https://doi.org/10.1007/s11063-024-11482-7

Hyperbolic Tangent-Type Variant-Parameter and Robust ZNN Solutions for Resolving Time-Variant Sylvester Equation in Preassigned-Time

Jiawei Luo[1,2] · **Lei Yu**[1,2] · **Bangshu Xiong**[1,2]

Accepted: 27 November 2023

Abstract
To solve a general time-variant Sylvester equation, two novel zeroing neural networks (ZNNs) solutions are designed and analyzed. In the foregoing ZNN solutions, the design convergent parameters (CPs) before the nonlinear stimulated functions are very pivotal because CPs basically decide the convergent speeds. Nonetheless, the CPs are generally set to be constants, which is not feasible because CPs are generally time-variant in practical hardware conditions particularly when the external noises invade. So, a lot of variant-parameter ZNNs (VP-ZNNs) with time-variant CPs have been come up with. Comparing with fixed-parameter ZNNs, the foregoing VP-ZNNs have been illustrated to own better convergence, the downside is that the CPs generally increases over time, and will be probably infinite at last. Obviously, infinite large CPs would lead to be non-robustness of the ZNN schemes, which are not permitted in reality when the exterior noises inject. Moreover, even though VP-ZNNs are convergent over time, the growth of CPs will waste tremendous computing resources. Based on these factors, 2 hyperbolic tangent-type variant-parameter robust ZNNs (HTVPR-ZNNs) have been proposed in this paper. Both the convergent preassigned-time of the HTVPR-ZNN and top-time boundary of CPs are theoretically investigated. Many numerical simulations substantiated the admirable validity of the HTVPR-ZNN solutions.

Keywords Hyperbolic tangent-type · Variant parameter · Zeroing neural network · Preassigned-time convergence · Time-variant Sylvester equation

✉ Jiawei Luo
luo_jia_wei@foxmail.com

Lei Yu
yulei@nchu.edu.cn

Bangshu Xiong
xiongbs@126.com

[1] School of Information Engineering, NanChang HangKong University, Nanchang 330063, China

[2] The Key Laboratory of Image Processing and Pattern Recognition, NanChang HangKong University, Nanchang 330063, China

Published online: 13 May 2024

1 Introduction

Generally, how to resolve the complex time-variant Sylvester equations (TVSEs) $A(t)X(t) - X(t)B(t) + C(t) = 0$, which is a basic mathematical question involved in many control systems and machine vision quests, with better disturbance rejection characters and faster convergence speed, has aroused more and more concern [1]. To resolve the corresponding design problems for dynamic nonlinear systems [2], switched nonlinear systems [3], time-delay systems [4] and stochastic nonlinear systems [5]. Many solutions have been put forward, such as Bartels–Stewart algorithm, homogeneous approach, terminal sliding mode control approach and so on [6].

These methods can get an ideal result with dealing with small dimensions Sylvester equations. But when the dimensions of Sylvester equations get larger, they will have a poor efficiency. With the development of technology, the neural-dynamic solutions have been applied in practice. Gradient neural networks (GNN) is one of the methods. However, the evolution speed of GNN may not synchronize with the change speed of time-variant coefficient. To solve this problem, zero neural network (ZNN), a kind of RNN, is proposed. ZNN owns many desired features, for instance higher accuracy, disturbance rejection features and faster convergent rate [7, 8]. Particularly, the main way for analysis of preassigned-time stability in the nonlinear situation is the Lyapunov function method [7–10]. With the purpose of accelerating the convergence, Weibing Li first used a sign-bi-power function stimulated ZNN that owns finite-time convergence [1–3]. Recently, ZNNs have been broadly applied to solve many time-variant questions under finite-time [11–14].

The ZNN solutions involve a design convergence parameter (CP) that influences the ZNNs convergent performance [15–18]. The CPs of conventional ZNNs are limited to be constants [19–21]. To obtain a better convergent performance, different variant-parameter ZNNs (VP-ZNNs) with time-variant CPs have been obtained [21–23]. The time-varying CPs shown in [24–26] can expedite the convergence of ZNNs, but the current CPs design results in two problems: (1) the CPs increase over time in the course of this solving process; and (2) it occupies too much computing resources.

Fixed-time convergence/stability was firstly proposed by Polyakov in 2012 to eliminate the dependence of the convergent time on initial values [27, 28]. This elimination has great advantages and convenience in applications compared to finite time stability, as the initial values of many real systems may not be accessible in advance [27–30]. Therefore, in the fields of power systems and space technology, fixed-time stability has received a lot of attention and become a hot research field [27–31]. Compared with the finite-time convergence, preassigned-time convergence does not depend on the initial states of ZNN; based on the known design parameters, the convergence-time's upper bound can be calculated beforehand [32–34]. Once preassigned-time convergence is reached, we also call it preassigned-time stable [33–36].

To solve the above problems, we propose the hyperbolic tangent-type variant-parameter robust ZNN (HTVPR-ZNN) solutions for resolving the time-variant Sylvester equations. The primary contributions of our work are as follow:

(1) To resolve the complex time-variant Sylvester equations, two new HTVPR-ZNN solutions are designed. Differing from the existing VP-ZNNs and FP-ZNNs, the HTVPR-ZNN involves hyperbolic tangent-type parameters that can be changed over time and also converge to a constant once the HTVPR-ZNN is convergent in preassigned time.
(2) Unlike other ZNN solutions, the proposed HTVPR-ZNN solutions employ two new nonlinear activation functions that own various variable parameters as well. The stability and robustness of the HTVPR-ZNN solutions are proven. Moreover, the preassigned-

time convergence upper bound of the HTVPR-ZNN is obtained, which is smaller than other convergence ZNN solutions.

(3) Comparative numerical simulations are done to demonstrate the excellent convergent characters of the HTVPR-ZNN solutions. Many stimulation functions are comparatively used to stimulate the HTVPR-ZNN solutions. The results theoretically illustrate that two HTVPR-ZNN solutions are effective to tackle the TVSEs under the interference of different noises (for instance the time-variant bounded constant noise). Moreover the preassigned time is calculated as a priority and independent of initial situations.

The structure of this article is as follows. In Sect. 2, we introduce the problem formulation and preliminary results. Section 3, we develop HTVPR-ZNN Solutions. Main theoretical analysis is shown in Sect. 4. One numerical simulation example is presented to prove the validity of solutions in Sect. 5. At last, a conclusion is put in Sect. 6.

2 Problem Formulation and Preliminaries

The time-variant Sylvester problem formulation and its preliminaries are described in this subsection. The design procedures of HTVPR-ZNN solutions and regularity condition (RC) for the solution of the TVSEs are illustrated as well [21, 22].

We consider a high smooth and rank matrix $A(t) \in \mathbb{R}^{m\times m}$, the problem of the TVSE is defined as

$$A(t)X(t) - X(t)B(t) = -C(t), \quad \forall t \in [0, +\infty) \tag{1}$$

$$M(t)X(t) = L(t), \tag{2}$$

while $X(t) \in \mathbb{R}^{m\times n}$ is an uncertain time-variant state matrix that neeeds to be resolved and t denotes the time variable. Then the time-variant coefficient matrices $A(t) = (a_{ij}(t))_{m\times m}$, $B(t) = (b_{ij}(t))_{n\times n}$, and $C(t) = (c_{ij}(t))_{m\times n}$ and the time derivatives matrices $\dot{A}(t)$, $\dot{B}(t)$ and $\dot{C}(t)$ are settled to be estimated. If this Sylvester equation is true, then the corresponding scheme $X(t) = X^*(t) \in \mathbb{R}^{m\times n}$ of the Sylvester equation holds, its reliable to figure out the right solution quickly.

Before the new HTVPR-ZNN solutions are raised to solve the upper Sylvester equation (1), two important lemmas are provided as follows.

Lemma 1 [37, 38] *We consider a nonlinear systems of the nether differential equations:*

$$\dot{x}(t) = h(t, x), x(0) = x_0 \tag{3}$$

where $h(0) = 0$, and $x = [x_1, x_2, \ldots, x_n]^T$, $h(t, x) : R^n \to R^n$ is a nonlinear function.

If there is a unbounded and radially continuous function $Q : R^n \to R^n$ with a result that

(1) *for every $x \in \mathbb{R}^n\backslash\{0\}$ there is $x \in R_+$ so that $Q(x) = 0$;*

(2) *then any solution x(t) of (3) satisfies the inequality:*

$$\dot{Q}(x(t)) \le -\alpha_1 Q^{\mu}(x(t)) - \beta_2 Q^{\nu}(x(t)),$$

where parameters $\alpha_1 > 0$, $\beta_2 > 0$, $0 \le \mu < 1$ and $\nu > 1$. The system is globally preassigned-time stable, then the upper bound of the settling time is:

$$T(x_0) = \frac{1}{\alpha_1(1-\mu)} + \frac{1}{\beta_2(\nu-1)}, \forall x_0 \in \mathbb{R}^n.$$

.

Lemma 2 *If any solution x(t) of (3) satisfies the inequality:*

$$\dot{Q}(x(t)) \leq -\beta_1 Q^p(x(t)) - \beta_2 Q^q(x(t)) - \beta_3 Q^r(x(t)),$$

where parameters $\beta_1, \beta_2, \beta_3 > 0$, $0 \leq q < 1$, $p, r > 1$. *The system is globally preassigned-time stable, and the upper boundary of the settling time is:*

$$T(x_0) = Max\left\{\frac{\ln\left[\frac{\beta_1+\beta_3}{\beta_3 Q(x(0))^{1-p}+\beta_1}\right]}{\beta_3(p-1)}, \frac{\ln\left[\frac{\beta_1+\beta_3}{\beta_1 Q(x(0))^{1-r}+\beta_3}\right]}{\beta_1(r-1)}\right\} + \frac{1}{\beta_2(1-q)}.$$

Proof For any x(t) so that Case I: $Q(x(0)) > 1$, the last inequality

$$\dot{Q}(x(t)) \leq -\beta_1 Q^p(x(t)) - \beta_3 Q^r(x(t)).$$

By classification, we have

$$\dot{Q}(x(t)) \leq \begin{cases} -(\beta_1+\beta_3)Q^p(x(t)), & p = r;\ (a) \\ -\beta_1 Q^p(x(t)) - \beta_3 Q^1(x(t)), & p > r > 1;\ (b) \\ -\beta_1 Q^1(x(t)) - \beta_3 Q^r(x(t)), & r > p > 1.\ (c) \end{cases}$$

Since situation (a) is similar to the situation in [29], we get

$$T(x_0) = \frac{1}{(\beta_1+\beta_3)(1-p)}, \quad \forall x_0 \in \mathbb{R}^n.$$

Then we focus on case situation (b) and multiply (b) by $\exp(\beta_3 t)$ yields,

$$e^{\beta_3 t}\dot{Q}(x(t)) + e^{\beta_3 t}\beta_3 Q(x(t)) \leq -e^{\beta_3 t}\beta_1 Q^p(x(t)).$$

Then,

$$\frac{\mathrm{d}e^{\beta_3 t}Q(t)}{(e^{\beta_3 t}Q(t))^p} \leq -\beta_1 e^{(1-p)\beta_3 t}\mathrm{d}t.$$

Integrating the above differential inequality from 0 to t, we can obtain

$$Q(x(t)) \geq e^{-\beta_3 t}\left[Q(x(0))^{1-p} + \frac{\beta_1}{\beta_3} - \frac{\beta_1}{\beta_3}e^{(1-p)\beta_3 t}\right]^{\frac{1}{1-p}},$$

let the upper right part equal to 1, we get t_1',

$$t_1' = \frac{\ln\left[\frac{\beta_1+\beta_3}{\beta_3 Q(x(0))^{1-p}+\beta_1}\right]}{\beta_3(p-1)},$$

such that $Q(x) \leq 1$,$t \geq t_1'$.

Similarly, with regard to (c) situation, we get

$$Q(x(t)) \geq e^{-\beta_1 t}\left[Q(x(0))^{1-r} + \frac{\beta_3}{\beta_1} - \frac{\beta_3}{\beta_1}e^{(1-r)\beta_1 t}\right]^{\frac{1}{1-r}},$$

let the upper right part equal to 1, we get t_1'',

$$t_1'' = \frac{\ln\left[\frac{\beta_1+\beta_3}{\beta_1 Q(x(0))^{1-r}+\beta_3}\right]}{\beta_1(r-1)},$$

while $Q(x) \leq 1, t \geq t_1''$.

Let $t_1 = Max(t_1', t_1'')$,

$$t_1 = Max\left\{\frac{\ln\left[\frac{\beta_1+\beta_3}{\beta_3 Q(x(0))^{1-p}+\beta_1}\right]}{\beta_3(p-1)}, \frac{\ln\left[\frac{\beta_1+\beta_3}{\beta_1 Q(x(0))^{1-r}+\beta_3}\right]}{\beta_1(r-1)}\right\}.$$

Then, for any x(t) such that $Q(x(t')) \leq 1$, the before inequality

$$\dot{Q}(x(t')) \leq -\beta_2 Q^q(x(t')), \quad t' \geq t_1,$$
$$t_2 = \frac{Q^{1-q}(t_1)}{\beta_2(1-q)} = \frac{1}{\beta_2(1-q)}.$$

So, we make $Q(x(t)) = 0$, for

$$t \geq t_1 + t_2 = \frac{\ln\left[\frac{\beta_1+\beta_3}{\beta_3 Q(x(0))^{1-p}+\beta_1}\right]}{\beta_3(p-1)} + \frac{1}{\beta_2(1-q)}.$$

Case II: Once $Q(x(0)) \leq 1$, the inequality

$$\dot{Q}(x(t)) \leq -\beta_2 Q^q(x(t)),$$

holds, indicates

$$t \geq \frac{1}{\beta_2(1-q)}, Q(x(t)) = 0.$$

Finally, $Q(x_0) \geq 1$ and $Q(x(t)) = 0$ for

$$\forall t \geq T(x_0) = Max\left\{\frac{\ln\left[\frac{\beta_1+\beta_3}{\beta_3 Q(x(0))^{1-p}+\beta_1}\right]}{\beta_3(p-1)}, \frac{\ln\left[\frac{\beta_1+\beta_3}{\beta_1 Q(x(0))^{1-r}+\beta_3}\right]}{\beta_1(r-1)}\right\} + \frac{1}{\beta_2(1-q)}.$$

Therefore, the system has globally predefined-time convergence/stability and its settling time satisfies the upper boundary. □

3 HTVPR-ZNN Solutons

In this part, through using two nonlinear activation functions we design and develop the HTVPR-ZNN solution for the specific Sylvester problem (1) [32–36].

Step 1: To survey the time-variant process, we define a matrix-type error function (EF) as

$$E(t) = A(t)X(t) - X(t)B(t) + C(t), \quad \forall t \in [0, +\infty). \tag{4}$$

The time-variant unique solution $X^*(t)$ of the TVSE (1) can be obtained once the error function (4) equals or converges to zero. Thus it successfully turns the initial problem (1) into insuring $E(Q(t), t)$ equals to 0.

Step 2: With the purpose of ensuring each element $e_{ij}(t)$ $(i = 1, 2, \ldots, m, j = 1, 2, \ldots, n)$ of $E(Q(t), t)$ convergent to 0, the EF derivation $\dot{E}(Q(t), t)$ is expressed as:

$$\frac{\mathrm{d}E(Q(t), t)}{\mathrm{d}t} = -\Lambda(t)F(E(Q(t), t)), \tag{5}$$

where $F(\cdot) : \mathbb{R}^{m\times n} \to \mathbb{R}^{m\times n}$ is a mapping of a matrix and every unit is a monotone increasing odd function. The Λ is a positive-defined matrix that influences the convergent speed of (5).

For the simplicity of theoretical analysis, Λ is set to γI, where $\gamma > 0$ and I is an identity matrix. Hence, each unit of $E(Q(t), t)$ owns the coincident convergence speed adjusted by parameter γ.

$$\Lambda(t) = \begin{bmatrix} \lambda_1(t) & 0 & \cdots & 0 \\ 0 & \lambda_2(t) & \ddots & 0 \\ \vdots & \vdots & \ddots & 0 \\ 0 & 0 & \cdots & \lambda_m(t) \end{bmatrix} \in \mathbb{R}^{m\times n}.$$
$$\lambda_i(t) = \gamma \tanh(|e(t)|/\epsilon)$$

Step 3: Combining Steps 1 and 2, then we obtain one consistent HTVP-ZNN solution for resolving Sylvester equation (1):

$$\begin{aligned} A(t)\dot{X}(t) + \dot{X}(t)B(t) = &-\dot{A}(t)X(t) - X(t)\dot{B}(t) - \dot{C}(t) \\ &- \Lambda(t)F(A(t)X(t) + X(t)B(t) + C(t)). \end{aligned} \tag{6}$$

where $F(\cdot)$ denotes 2 new stimulation functions (i.e., PpSAF and NSBPAF).

With the injection of noise, the perturbed HTVPR-ZNN solution is obtained as follows:

$$\begin{aligned} A(t)\dot{X}(t) + \dot{X}(t)B(t) = &-\dot{A}(t)X(t) - X(t)\dot{B}(t) - \dot{C}(t) \\ &- \Lambda(t)F(A(t)X(t) + X(t)B(t) + C(t)) + N(t). \end{aligned} \tag{7}$$

where $N(t) \in \mathbb{R}^{m\times n}$ denotes external noise. After dealing with the upper equation, the column vectorization of HTVPR-ZNN solution (7) can be deduced as

$$M(t)\dot{X}(t) = -\dot{M}(t)X(t) - \dot{C}(t) - \Lambda(t)F(E(t)) + N(t), \tag{8}$$

where $M(t) := I^{m\times m} \otimes A(t) + B^T(t) \otimes I^{n\times n}$, $X(t) := \mathrm{vec}(\dot{X}(t))$, $e(t) := M(t)X(t) - \mathrm{vec}(C(t))$, and $N(t) := \mathrm{vec}(N(t))$. Our goal of this paper is to propose two new solutions for systems (1) so that the corresponding closed-loop system owns fast preassigned-time convergence.

3.1 Different Stimulation Functions

Stimulation functions (SFs) play very vital roles in the ZNN solutions. Different stimulation functions are adopted to ZNN solutions with many results. When the ZNN solutions stimulated by SBPAF achieving finite-time convergence [1, 2]. And their finite-time convergence is mainly influenced by the initial conditions of ZNN solution, which lead it very difficult to find out the upper boundary because of the undiscovered initial condition [26, 39, 40]. In this paper, four conventional SFs and two new SFs have been adopted to stimulate the proposed ZNN solutions:

(1) Linear function (LF): $F(x) = d \cdot x$.

(2) Smooth power-sigmoid function (SPSF):

$$F(x) = \frac{1}{2}\left(\frac{1-\exp(-bx)}{1+\exp(-bx)} \cdot \frac{1+\exp(-b)}{1-\exp(-b)+x^a}\right), \quad \text{where } a \geq 3, \quad b > 2.$$

(3) Power-sigmoid function (PSF):

$$F(x) = \begin{cases} x^p, & if\ |x| \geq 1, \\ \frac{1+\exp(-b)}{1-\exp(-b)} \cdot \frac{1-\exp(-bx)}{1+\exp(-bx)}, & otherwise, \end{cases}$$

(4) Sign-bi-Power function (SBPF):

$$F(x) = \frac{1}{2}|x|^{\iota}\operatorname{sign}(x) + \frac{1}{2}|x|^{\frac{1}{\iota}}\operatorname{sign}(x)$$
$$\text{where } 0 < \iota < 1.$$

Consider the features of different SFs, let's induce it into the HTVPR-ZNN solution to resolve the TVSEs achieving the preassigned-time convergence. The expression of PpSAF can be:

$$F(u) = \left(\beta_1 \operatorname{sign}(u) + \beta_2 u^p\right), \tag{9}$$

When $\beta_1 = 1$ and $\beta_2 = 1$, (9) will be $F(u) = \operatorname{sign}(u) + u^p$, odd $p >= 3$.

Referring to previous works [34–36, 40], we come up with a new sign-bi-Power activation function (NSBPAF), which will be convergent in a preassigned time. Its formula is presented as follow:

$$F_1(u) = \left(\beta_1 |u|^p + \beta_2 |u|^q\right)\operatorname{sign}(u) + \beta_3 u^r + \beta_4 \operatorname{sign}(u), \tag{10}$$

where design parameters $\beta_1 > 0$, $\beta_2 > 0$, $\beta_3 \geq 0$, $\beta_4 \geq 0$, $p > 1$, $0 < q < 1$, $r = 1, 3, 5$ and $\operatorname{sign}(\cdot)$ represents signum function. Initial parts $(\beta_1|u|^p + \beta_2|u|^q)\operatorname{sign}(u)$ are used to obtain the preassigned-time convergence; Then time-variant boundary constant noises can be repressed by the intermittent items $\beta_3 u^r$ and $\beta_4 \operatorname{sign}(u)$.

For convenience, the HTVPR-ZNN solutions stimulated by PpSAF and NSBPAF are respectively called HTVPR-ZNN1 and HTVPR-ZNN2 solution.

4 Main Theoretical Analysis

In this subsection, we will address the preassigned-time convergence of proposed HTVPR-ZNN solutions in 2 situations. By analysis, the preassigned-time convergence and also the robustness of HTVPR-ZNN solutions for solving TVSEs is illustrated rigorously.

4.1 Pure-Case1: Without Noises

Under the pure-case1: with no noises, we find the preassigned-time and robust convergence of the HTVPR-ZNN solutions for solving time-variant and non-linear equations.

Theorem 1 *Under pure environment, when PpSAF is adopted in HTVPR-ZNN1 solution, the state matrix $P(t)$ of HTVPR-ZNN1 solution beginning from random $P(0) \in \mathbb{R}^{m1\times n1}$ can converge to theoretical $P^*(t)$ in a preassigned-time T gradually:*

$$T \leq \frac{1}{\gamma\beta_1(1-q)} + \frac{1}{\gamma\beta_2(p-1)}.$$

Though Eqs. (4) and (5), we use an EF $\dot{E}(t) = -\lambda F(E(t))$. Then the subelement $\dot{\epsilon}(t) = -\lambda f(\epsilon(t))$, and $f(\cdot)$ is a common unit of $F(\cdot)$ are got. Using the Lyapunov theory, we

introduce a Lyapunov energy-function (LEF) $Nov(t) = |\epsilon(t)|$. When PpSAF is invasive, the formula of $\dot{N}ov(t)$ can be obtained as below:

$$\begin{aligned}\dot{N}ov(t) &= \frac{\mathrm{d}Nov(t)}{\mathrm{d}t} = \dot{\epsilon}(t)\mathrm{sign}(\epsilon(t)) \\ &= -\lambda f(\epsilon(t))\mathrm{sign}(\epsilon(t)) \\ &= -\gamma \tanh(|e(t)|/\epsilon)\left(\beta_1 \mathrm{sign}(\epsilon(t)) + \beta_2 \epsilon(t)^p\right)\mathrm{sign}(\epsilon(t)) \\ &= -\gamma \tanh(|e(t)|/\epsilon)\left(\beta_1 + \beta_2 \epsilon(t)^p \mathrm{sign}(\epsilon(t))\right) \\ &= -\gamma \tanh(|e(t)|/\epsilon)\left(\beta_1 + \beta_2 |\epsilon(t)|^p\right) \\ &\le -\gamma \tanh(|e(t)|/\epsilon)\left(\beta_1 |\epsilon(t)|^q + \beta_2 |\epsilon(t)|^p\right) \\ &= -\gamma \tanh(|e(t)|/\epsilon)\left(\beta_1 Nov^q(t) + \beta_2 Nov^p(t)\right).\end{aligned}$$

On account of the Lemma 1, the scheme for the upper LEF inequality can be

$$t \le \frac{1}{\gamma \tanh(|e(t)|/\epsilon)}\left(\frac{1}{\beta_1 (p-1)} + \frac{1}{\beta_2 (1-q)}\right).$$

Generally, the convergent time hinges on the trial parameters. Once the trial parameters are fixed, $T = \max(t)$ can be preassigned, the convergent time of HTVPR-ZNN1 solution

$$\begin{aligned}T_{\max}(t) &\le \frac{1}{\gamma \tanh(|e(t)|/\epsilon)}\left(\frac{1}{\beta_1 (1-q)} + \frac{1}{\beta_2 (p-1)}\right) \\ &\quad (0 \le \tanh(|e(t)|/\epsilon) \le 1) \\ &\le \frac{1}{\gamma}\left(\frac{1}{\beta_1 (1-q)} + \frac{1}{\beta_2 (p-1)}\right).\end{aligned} \tag{11}$$

make parameters $\beta_1 = 1$, $\beta_2 = 1$; $\gamma = 0.5, 1, 2, 3, \ldots$, $p = 3$ and $q = 0$; we have

$$T_{\max}(t) < \frac{1}{\gamma} + \frac{1}{2\gamma} = \frac{1.5}{\gamma}.$$

Finally, all the processes and steps show the preassigned-time convergence of HTVPR-ZNN1 solution stimulated by PpSAF for resolving the Sylvester equation (1).

Theorem 2 *Under pure environment, when NSBPAF is invasive in HTVPR-ZNN2 solution, the matrix $V(t)$ of HTVPR-ZNN2 solution beginning from $V(0) \in \mathbb{R}^{m\times n}$ will converge to theoretical $V^*(t)$ under preassigned-time T:*

$$T \le Max\left\{\frac{\ln\left[\frac{\beta_1+\beta_3}{\beta_3 Q(x(0))^{1-p}+\beta_1}\right]}{\beta_3(p-1)}, \frac{\ln\left[\frac{\beta_1+\beta_3}{\beta_1 Q(x(0))^{1-r}+\beta_3}\right]}{\beta_1(r-1)}\right\} + \frac{1}{\beta_2(1-q)}$$

Proof In Eqs. (4) and (5), we let an EF $\dot{E}(t) = -\gamma F(E(t))$. When NSBPAF is invasive, the formula of $\dot{N}ov(t)$ can be obtained as below:

$$\begin{aligned}\dot{N}ov(t) &= \frac{\mathrm{d}Nov(t)}{\mathrm{d}t} = \dot{\epsilon}(t)\mathrm{sign}(\epsilon(t)) = -\lambda(t) f(\epsilon(t))\mathrm{sign}(\epsilon(t)) \\ &= -\gamma \tanh(|e(t)|/\epsilon)\left(\beta_1 |\epsilon(t)|^p + \beta_2 |\epsilon(t)|^q + \beta_3 |\epsilon(t)|^r + \beta_4\right) \\ &\le -\gamma \tanh(|e(t)|/\epsilon)\left(\beta_1 |\epsilon(t)|^p + \beta_2 |\epsilon(t)|^q + \beta_3 |\epsilon(t)|^r\right) \\ &= -\gamma \tanh(|e(t)|/\epsilon)\left(\beta_1 Nov^p(t) + \beta_2 Nov^q(t) + \beta_3 Nov^r(t)\right).\end{aligned}$$

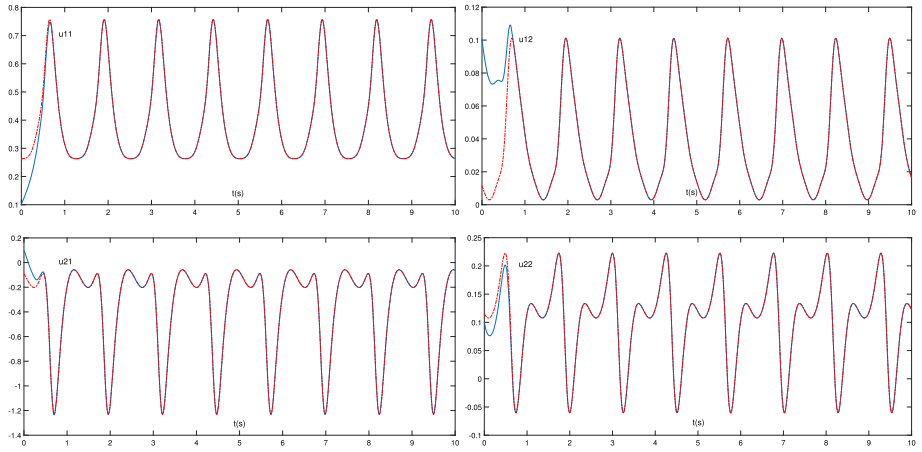

Fig. 1 Theoretical and analytical trajectories of Sylvester (1), where blue lines represent the process resolution of HTVP-ZNN solution (6) stimulated by PpSAF and the red represent the theory resolution of Sylvester (1). (Color figure online)

Based on the Lemma 2, then we get

$$\begin{aligned} t \leq & \frac{1}{\gamma \tanh(|e(t)|/\epsilon)} \\ & \left(Max \left\{ \frac{\ln\left[\frac{\beta_1+\beta_3}{\beta_3 Q(x(0))^{1-p}+\beta_1}\right]}{\beta_3(p-1)}, \frac{\ln\left[\frac{\beta_1+\beta_3}{\beta_1 Q(x(0))^{1-r}+\beta_3}\right]}{\beta_1(r-1)} \right\} + \frac{1}{\beta_2(1-q)} \right) \\ \leq & \frac{1}{\gamma} \left(Max \left\{ \frac{\ln\left[\frac{\beta_1+\beta_3}{\beta_3 Q(x(0))^{1-p}+\beta_1}\right]}{\beta_3(p-1)}, \frac{\ln\left[\frac{\beta_1+\beta_3}{\beta_1 Q(x(0))^{1-r}+\beta_3}\right]}{\beta_1(r-1)} \right\} + \frac{1}{\beta_2(1-q)} \right). \end{aligned} \tag{12}$$

Evidently the upper threshold of convergent time is preassigned and relied on the trial parameters. Make the parameters $\beta_1 = \beta_2 = \beta_3 = 1$; $\gamma = 0.5, 1, 2, \ldots$, $p = r = 3$, $q = 1/3$ and $Q(x_0) \geq 1$; then, we have

$$t \leq \frac{1}{\gamma} \left(Max \left\{ \frac{\ln\left[\frac{2}{Q(x(0))^{(-2)}+1}\right]}{2}, \frac{\ln\left[\frac{1}{Q(x(0))^{(-2)}+1}\right]}{2} \right\} + 1.5 \right). \tag{13}$$

□

4.2 Case2: Time-Variant Boundary-Constant Noise

When the boundary time-variant and constant noise is considered, every entry $n_{ij}(t)$ satifies the inequation $|n_{ij}(t)| \leq N + \delta$, whie $\delta \in (0, +\infty)$; and the convergent peculiarity of HTVPR-ZNN solutions under preassigned time is investigated.

Theorem 3 *When the bounded time-variant and constant noise is interferential, if PpSAF is used in HTVPR-ZNN1 solution with* $\beta_1 \gamma \tanh(|e(t)|/\epsilon) \geq N + \delta$, *the state matrix* $P(t)$

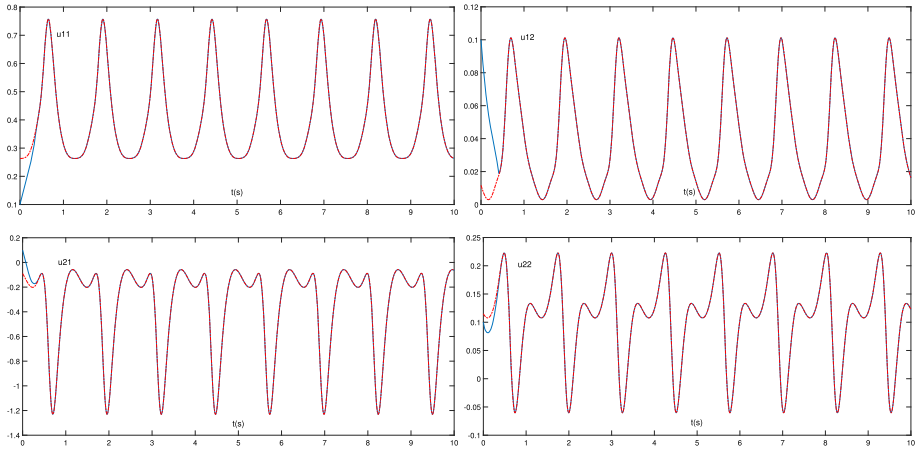

Fig. 2 Theoretical and analytical trajectories of Sylvester (1), where blue lines represent the process resolution of HTVP-ZNN solution (6) stimulated by NSBPAF and the red represent the theory resolution of Sylvester (1). (Color figure online)

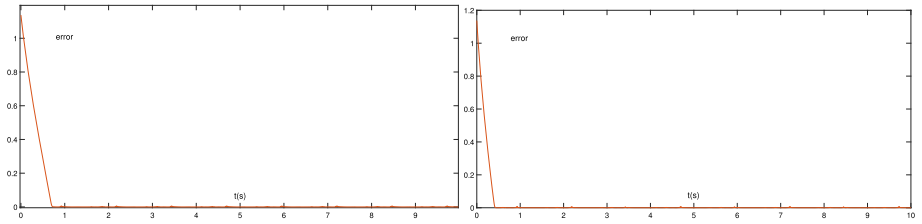

(a) (b)

Fig. 3 Steady-state residual errors of HTVP-ZNN solution (6) with no noise and r = 1. **a** By PpSAF. **b** By NSBPAF

of HTVPR-ZNN1 solution beginning from random $P(0) \in \mathbb{R}^{m1\times n1}$ *can slowly converge to theoretical* $P^*(t)$ *under the preassigned-time* T*:*

$$T \leq \frac{1}{(\gamma\beta_1 - (N+\delta))(1-q)} + \frac{1}{\gamma\beta_2(p-1)}.$$

Induce a LEF $Nov(t) = |\epsilon(t)|^2$, let's compute the $\dot{N}ov(t)$:

$$\begin{aligned}
\dot{N}ov(t) &= 2\epsilon(t)\dot{\epsilon}(t) = 2\epsilon(t)(-\lambda f(\epsilon(t)) + n(t)) \\
&= -2\lambda\epsilon(t)\left(\beta_1 \text{sign}(\epsilon(t)) + \beta_2\epsilon(t)^p\right) + 2\epsilon(t)n(t) \\
&= -2\gamma\tanh\left(|e(t)|/\epsilon\right)\left(\beta_1|\epsilon(t)| + \beta_2|\epsilon(t)|^{p+1}\right) + 2\epsilon(t)n(t) \\
&\leq -2\gamma\tanh(|e(t)|/\epsilon)\left(\beta_1|\epsilon(t)| + \beta_2|\epsilon(t)|^{p+1}\right) + 2|\epsilon(t)|(N+\delta) \\
&\quad \text{(when } \beta_1\gamma\tanh(|e(t)|/\epsilon) \geq N+\delta) \\
&= -2\gamma\tanh(|e(t)|/\epsilon)\left((\beta_1 - (N+\delta)/\gamma)|\epsilon(t)| + \beta_2|\epsilon(t)|^{p+1}\right) \\
&= -2\gamma\tanh(|e(t)|/\epsilon)\left((\beta_1 - (N+\delta)/\gamma)Nov^{\frac{q+1}{2}}(t) + \beta_2 Nov^{\frac{q+1}{2}}(t)\right).
\end{aligned}$$

Then, we get the restringent time of contaminated HTVPR-ZNN1 solution:

$$\begin{aligned} T_{\max}(t) &\leq \frac{1}{(\gamma \tanh(|e(t)|/\epsilon)\beta_1 - (N+\delta))(1-q)} + \frac{1}{\gamma \tanh(|e(t)|/\epsilon)\beta_2(p-1)} \\ &\quad (0 \leq \tanh(|e(t)|/\epsilon) \leq 1) \\ &\leq \frac{1}{(\gamma\beta_1 - (N+\delta))(1-q)} + \frac{1}{\gamma\beta_2(p-1)}. \end{aligned} \tag{14}$$

Set $\beta_1 = 1$, $\beta_2 = 1$; $\gamma = 1, 1.5, 2, \ldots$, $p = 3$ and $q = 0$; there is

$$T_{\max}(t) \leq \frac{1}{(\gamma - (N+\delta))} + \frac{1}{2\gamma}. \tag{15}$$

Theorem 4 *When the noise is invasive, once NSbpAF is used in the polluted HTVPR-ZNN2 solution with $\beta_4 \tanh(|e(t)|/\epsilon) \geq \delta$, $Q(t)$ of HTVPR-ZNN2 solution beginning from $Q(0) \in \mathbb{R}^{m\times n}$ can converge to theoretical $Q^*(t)$ under preassigned-time.*

Proof Bring in a LEF $Nov(t) = |\epsilon(t)|^2$, let's compute the $\dot{Nov}(t)$:

$$\begin{aligned} \dot{Nov}(t) &= 2\epsilon(t)\dot{\epsilon}(t)(t) = 2\epsilon(t)(-\lambda f(\epsilon(t)) + n(t)) \\ &= -2\gamma\left(\beta_1|\epsilon(t)|^{p+1} + \beta_2|\epsilon(t)|^{q+1} + \beta_3|\epsilon(t)|^{r+1}\right) \\ &\quad + 2(\epsilon(t)n(t) - \gamma\beta_4|\epsilon(t)|) \\ &\leq -2\gamma\left(\beta_1|\epsilon(t)|^{p+1} + \beta_2|\epsilon(t)|^{q+1} + \beta_3|\epsilon(t)|^{r+1}\right) \\ &\quad + 2((N+\delta)|\epsilon(t)| - \gamma\beta_4|\epsilon(t)|) \\ &\leq -2\gamma\left(\beta_1|\epsilon(t)|^{p+1} + \beta_2|\epsilon(t)|^{q+1} + \beta_3|\epsilon(t)|^{r+1}\right) \\ &= -2\gamma\left(\beta_1 Nov^{\frac{p+1}{2}}(t) + \beta_2 Nov^{\frac{q+1}{2}}(t) + \beta_3 Nov^{\frac{r+1}{2}}(t)\right). \end{aligned}$$

From Lemma 2, it can be concluded that the convergent time of the contaminated HTVPR-ZNN2 solution is also preassigned. □

Remark 1 It can be seen from Theorems 1 and 2 that there exists a preassigned-time convergent peculiarity of the HTVPR-ZNN1 and the HTVPR-ZNN2 solutions in pure environment, based on the known design parameters, the convergence-time's upper bound can be calculated beforehand. Then, seen from the convergence time of two HTVPR-ZNN solutions presented in (11) and (13). Then the convergence speed of HTVPR-ZNN2 solution will be faster than that of HTVPR-ZNN1 solution.

Remark 2 Seen from the Theorems 3 and 4, the 2 polluted HTVPR-ZNN solutions can converge to the theoretical solution of TVSE (1) under preassigned time. And they also suppress the time-variant bounded constant noise very well under the noised environment.

Remark 3 From the above design procedure, we know that two HTVPR-ZNN solutions with PpSAF and NSBPAF bring lots of parameters: β_i ($i = 1, 2, 3, 4$), p, q and r; they determine the peculiarity of HTVPR-ZNN solutions. Theorems 1 and 2 illustrate that HTVPR-ZNN1 solution stimulated by PpSAF, its convergence time is contingent on γ, β_1, β_2, p. When HTVPR-ZNN2 solution stimulated by NSBPAF, its convergence time is determined by the γ, β_1, β_2, β_3, β_4, p, q and r. Seen from Theorems 3 and 4, coefficients β_3 and β_4 would suppress the invasive noises. In addition, their parameters β_1 and β_2 are used to tolerate various noises respectively. Increasing the value of γ, all the preassigned-time T will be much smaller.

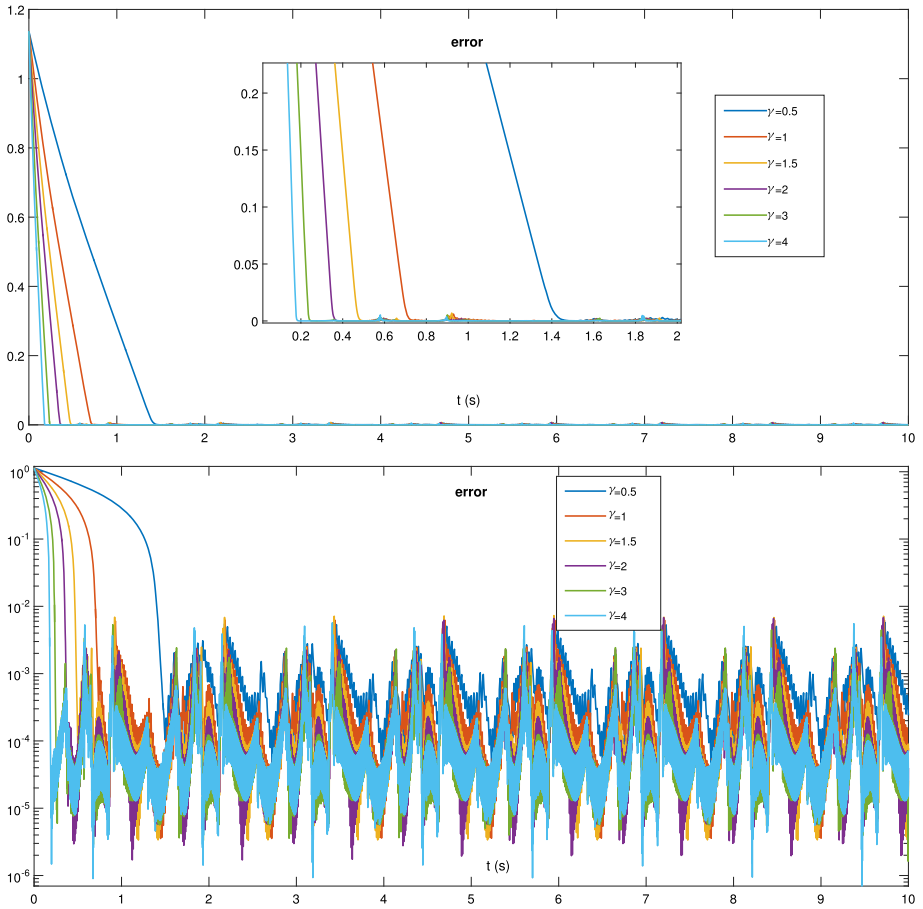

Fig. 4 Errors of HTVP-ZNN1 solution (6) stimulated by PpSAF to resolve the time-variant Sylvester (1) with the six values of the parameter γ

5 Numerical Simulation Example

One example is provided in this section on dealing with the TVSE (1). We apply the 2 HTVPR-ZNN solutions to prove the validity of the our theorems.

Firstly, We bring in the coefficient matrices of Sylvester equation as below:

$$A(t) = \begin{bmatrix} 3c^2/2 - 1 & -3s/4 - 1 \\ -3s/4 + 1 & 3s^2/2 - 1 \end{bmatrix},$$
$$C(t) = \begin{bmatrix} 2s - 3sc^2 & -c(1 - 6s^2)/2 \\ c(4 - 3c^2 + 3s^2)/2 & s(1 - 3s^2 + 3c^2)/2 \end{bmatrix},$$

while $s = sin(5t)$, $c = cos(5t)$. The theoretical solution can be:

$$P^*(t) = \begin{bmatrix} \sin(5t) & -\cos(5t) \\ \cos(5t) & \sin(5t) \end{bmatrix},$$

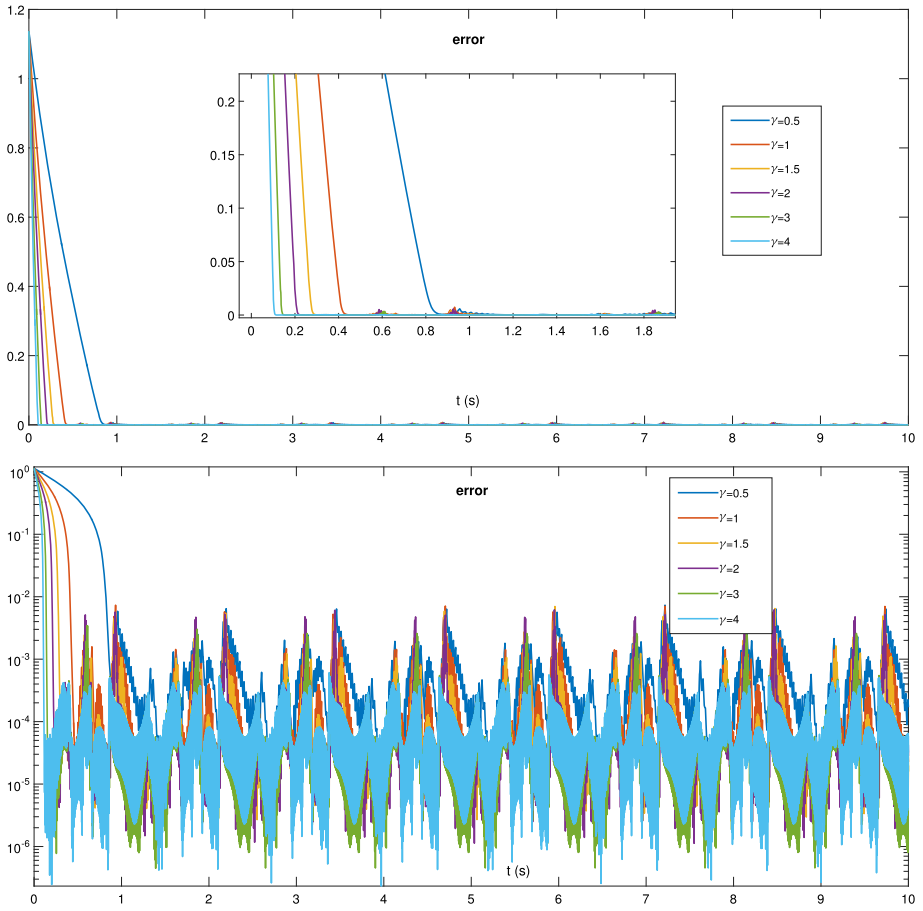

Fig. 5 Errors of HTVP-ZNN2 solution (6) stimulated by NSBPAF to resolve the time-variant Sylvester (1) with the six values of the parameter γ

which settles a basis to prove the availability of our proposed solutions.

$$N(t) = \begin{bmatrix} \sin(10t) & 2+\cos(10t) \\ 1+\cos(10t) & -\sin(10t) \end{bmatrix},$$

which is used as a invasive noise to verify the robustness of our proposed solutions.

Under the pure environment, the convergence time of our proposed solutions can be predicted and preassigned. Figures 1 and 2 exhibit the moving trajectories of TVSE (1) respectively stimulated by PpSAF and NSBPAF. Seen from Fig. 3a, the solution (6) stimulated by PpSAF, $\gamma = 1$ the corresponding convergent time $T \leq 0.61$ s; and $T \leq 0.42$ s when stimulated by NSBPAF. The residual errors presented in following figures also verify the truth, which proves the effectiveness of the Theorems 1 and 2 further.

Figure 4 shows the corresponding errors of HTVPR-ZNN1 solution stimulated by PpSAF to resolve the TVSE(1) with 6 different values of γ. And Fig. 5 displays the corresponding errors of HTVPR-ZNN2 solution stimulated by NSBPAF to resolve the TVSE(1) with the six different values of γ ($\gamma = 0.5$, $\gamma = 1$, $\gamma = 1.5$, $\gamma = 2$, $\gamma = 3$ and $\gamma = 4$). Moreover,

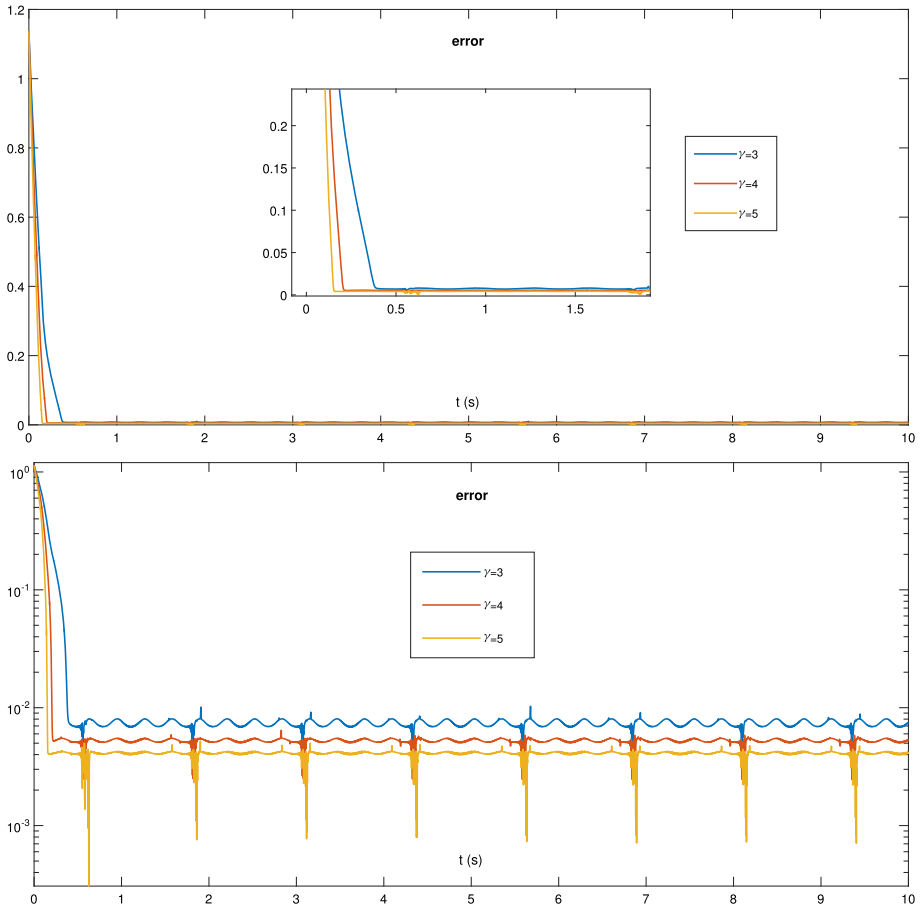

Fig. 6 Errors of disturbed HTVPR-ZNN1 solution (7) stimulated by PpSAF to resolve the time-variant Sylvester (1) with 3 values of γ

seen from Figs. 4 and 5, HTVPR-ZNN2 solution has more quickly convergent speed than HTVPR-ZNN1 solution, in the matter of errors.

Figures 6 and 7 adopt the time-variant boundary constant noise refer to the inescapability of distruction. HTVPR-ZNN solutions own nearly the uniform convergence time. However, when stimulated by linear, smooth power-sigmoid, power-sigmoid and SBPAF, the convergent delays of time seriously. And the corresponding errors of HTVPR-ZNN solutions can converge to zero as usual, while the errors of stimulation functions such as linear, Smooth power-sigmoid, power-sigmoid and SBPAF cannot converge to 0 and merely provide the upper boundaries. Numerical experiments results prove the effectiveness of preassigned-time convergence theory from Theorems 1–4. Moreover, NSbpAF do better than others, which ulteriorly bears out the admirable noise-tolerance character of HTVPR-ZNN solutions.

In general, HTVPR-ZNN solutions' parameters play important roles in the numerical experiment simulations. And the influence of 3 parameters in simulations are presented in the Figs. 6 and 7. Then, the error would draw to 0 bit by bit. By fixing parameters $\beta_1 = \beta_2 = \beta_3 = \beta_4 = 1$, $p = 4$, $q = 0.25$ and $r = 3$, and convergence time of the proposed solution

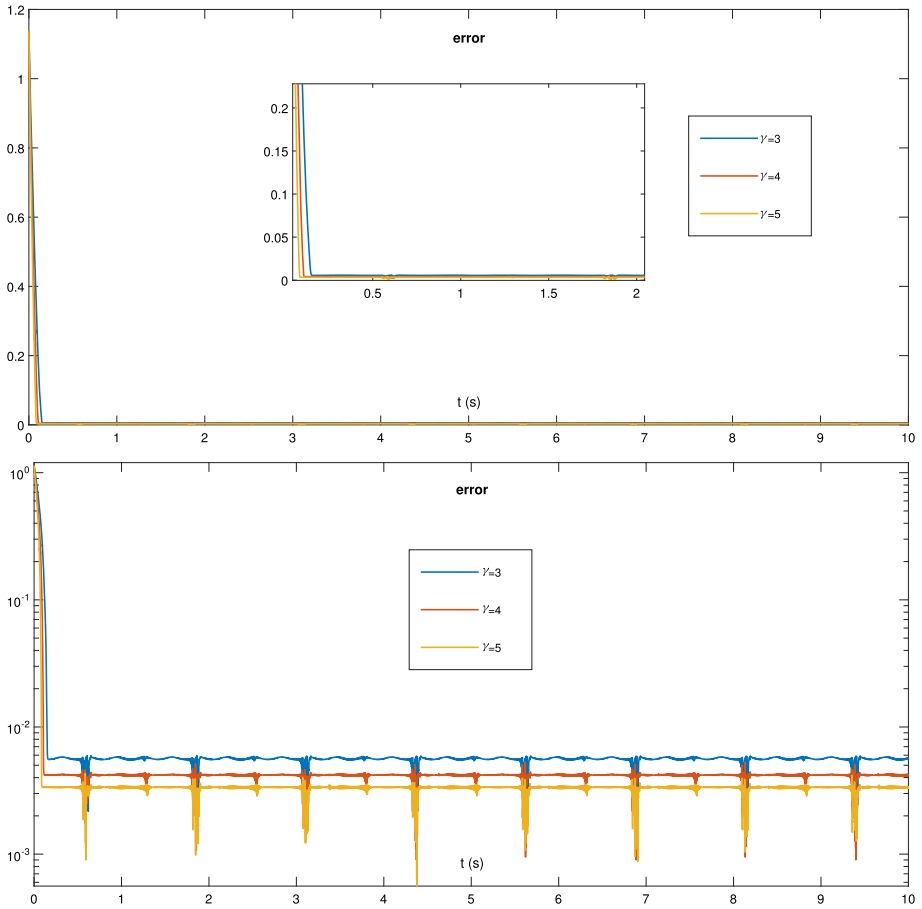

Fig. 7 Errors of disturbed HTVPR-ZNN2 solution (7) stimulated by NSBPAF to resolve the time-variant nonlinear Sylvester (1) with the 3 values of γ

(6) stimulated by PpSAF and NSbpAF are depend on γ. Then in later simulations, we adjust 3 various values ($\gamma = 3$, $\gamma = 4$ and $\gamma = 5$). Counting the convergent time, they will be smaller as we increase increase the value of the parameter γ.

To be specific, to further present the remarkable peculiarity of the proposed solution (6) with PpSAF and NSBPAF, other AFs involving Linear AF, SPSAF, BSAF, PSAF and SBPAF are used in the simulations too. Seen from the Fig. 8, the errors of PpSAF or NSBPAF converge to 0 more quickly than others. Furthermore HTVPR-ZNN2 solution has the fastest speed while HTVPR-ZNN1 solution is in the second place.

To improve the precision of the experimental results, we can adjust and set the values of the ODE45 solver. From Figs. 5, 6, 7 and 8, the relative and absolute error tolerances of the ODE45 solver are respectively preset as default values of 10^{-3} and 10^{-6}. Seen from the Fig. 9, the experimental results HTVPR-ZNN solutions errors become much smaller when decrease the RelTol and AbsTol values of the ODE45 solver (values of 10^{-4} and 10^{-8}). So the setting of ODE45 play important roles on the numerical experiment simulations. In

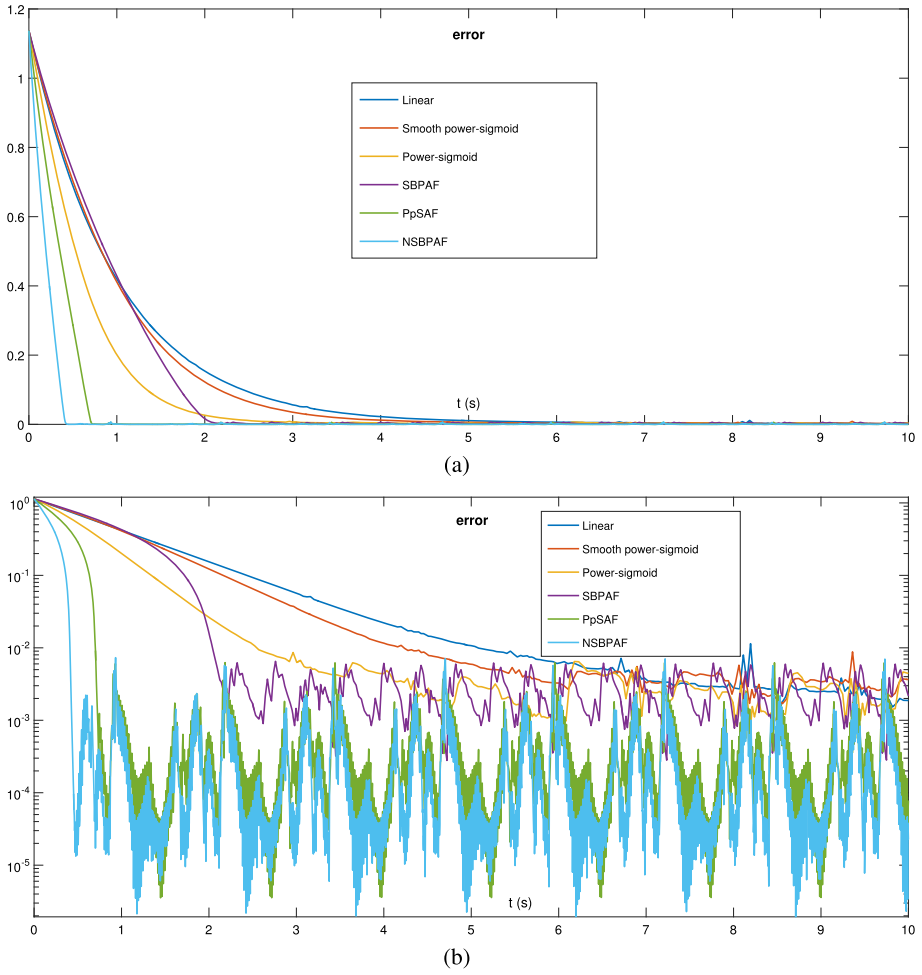

Fig. 8 Errors of HTVP-ZNN solution (6) stimulated by various functions

this case, its convergence time is the same; its setting time is mainly related to the design parameters.

In summary, all the results of simulations show that the 2 HTVPR-ZNN solutions have outstanding advantages. Moreover, facing with time-variant boundary-constant noise, both the 2 HTVPR-ZNN solutions maintain valid.

6 Conclusion

In the paper, 2 HTVPR-ZNN solutions for the time-variant Sylvester equation are come up with. HTVPR-ZNN has hyperbolic tangent-type parameters that can change over time; they will be constant when the HTVPR-ZNN are convergent at last. HTVPR-ZNN owns faster convergence than others such as FP-ZNNs. Global and preassigned-time convergence properties of HTVPR-ZNN solutions are proved theoretically. A number of simulations sub-

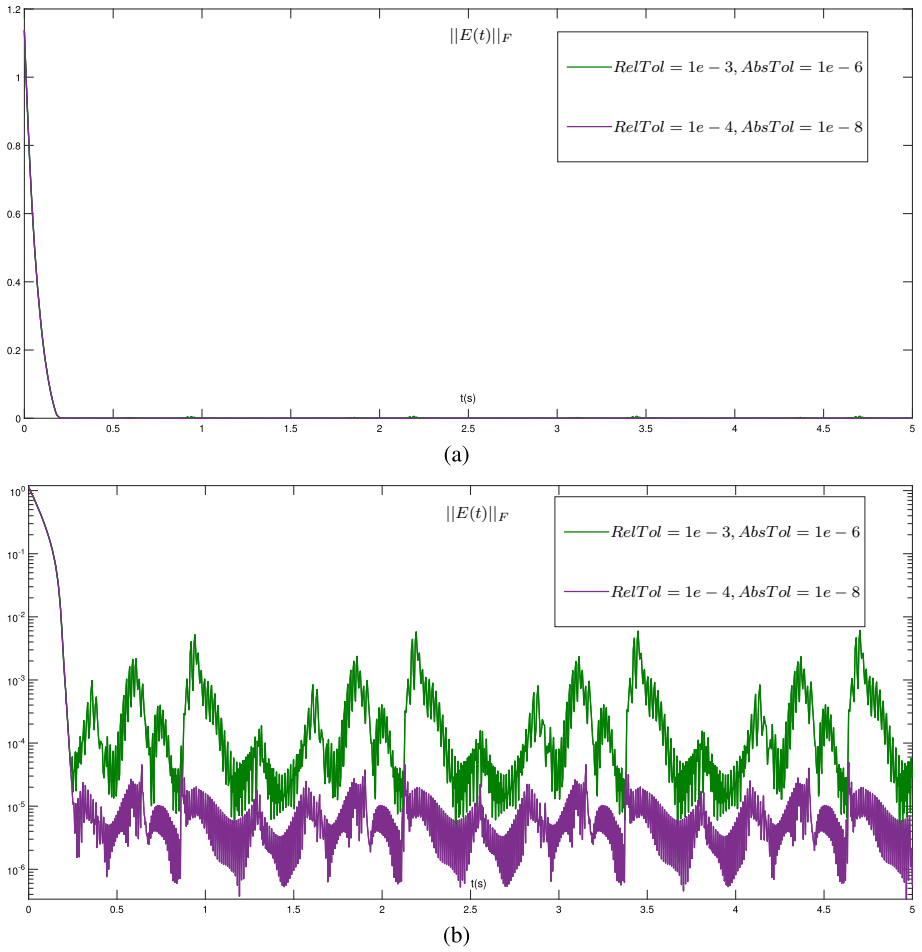

Fig. 9 Errors of solution (6) with the adjustments of the ODE45 solver when $\gamma = 1$

stantiate the accuracy and efficacy of HTVPR-ZNN solutions. Besides, we also study the influences of the related parameters and stimulation functions in the HTVPR-ZNN related to the convergence. In addition, the HTVPR-ZNN solutions can achieve an expedited convergence speed and reduce the assigned time. What's more, one example is further presented to indicate the effectiveness of our designed solutions intuitively. One of our future research efforts is to apply the HTVPR-ZNN solutions to some engineering situations such as robot manipulators' control.

Acknowledgements This work was supported by the National Natural Science Foundation of China (NSFC) under Grants (62162044), the Jiangxi Key Research and Development Plan under Grants (20212BBE53017) and the Aeronautical Science Foundation under Grants (20200057056006).

Author Contributions JL: conceptualization, methodology, software, validation, investigation, writing-original draft, project administration. LY: resources, writing-review and editing, supervision, funding acquisition. BX: software, supervision, investigation, validation, funding acquisition. All authors reviewed the manuscript.

Declarations

Conflict of interest The authors declare no competing interests.

References

1. Li W (2018) A recurrent neural network with explicitly definable convergence time for solving time-variant linear matrix equations. IEEE Trans Ind Inform 14(12):5289–5298
2. Li W, Ma X, Luo J, Jin L (2021) A strictly predefined-time convergent neural solution to equality- and inequality-constrained time-variant quadratic programming. IEEE Trans Syst Man Cybern 51(7):4028–4039
3. Li W, Xiao L, Liao B (2020) A finite-time convergent and noise-rejection recurrent neural network and its discretization for dynamic nonlinear equations solving. IEEE Trans Cybern 50(7):3195–3207
4. Zhang Z, Zheng L, Yang H, Qu X (2019) Design and analysis of a novel integral recurrent neural network for solving time-varying Sylvester equation. IEEE Trans Cybern 16(6):1477–1490
5. Chen D, Zhang Y (2018) Robust zeroing neural-dynamics and its time-varying disturbances suppression model applied to mobile robot manipulators. IEEE Trans Neural Netw Learn Syst 29(9):4385–4397
6. Liao B, Wang Y, Li W et al (2021) Prescribed-time convergent and noise-tolerant Z-type neural dynamics for calculating time-dependent quadratic programming. Neural Comput Appl 33:5327–5337
7. Liao B, Han L, He Y et al (2022) Prescribed-time convergent adaptive ZNN for time-varying matrix inversion under harmonic noise. Electronics 11(10):1636
8. Xiao L, Li S, Li K, Jin L, Liao B (2018) Co-design of finite-time convergence and noise suppression: a unified neural model for time varying linear equations with robotic applications. IEEE Trans Syst Man Cybern Syst 50(12):5233–5243
9. Qiu B, Guo J, Li X, Zhang Z, Zhang Y (2020) Discrete-time advanced zeroing neurodynamic algorithm applied to future equality-constrained nonlinear optimization with various noises. IEEE Trans Cybern 52(5):3539–3552
10. Li S, Chen S, Liu B (2013) Accelerating a recurrent neural network to finite-time convergence for solving time-varying Sylvester equation by using a sign-bi-power activation function. Neural Process Lett 37:189–205
11. Xiao L, Zhang Y (2014) From different Zhang functions to various ZNN models accelerated to finite-time convergence for time-varying linear matrix equation. Neural Process Lett 39:309–326
12. Li W, Su Z, Tan Z (2019) A variable-gain finite-time convergent recurrent neural network for time-variant quadratic programming with unknown noises endured. IEEE Trans Ind Inform 15(9):5330–5340
13. Zhang Y, Zhang Y, Chen D, Xiao Z, Yan X (2016) From Davidenko method to Zhang dynamics for nonlinear equation systems solving. IEEE Trans Syst Man Cybern 99:1–14
14. Jin L, Zhang Y, Qiao T, Tan M, Zhang Y (2016) Tracking control of modified Lorenz nonlinear system using ZG neural dynamics with additive input or mixed inputs. Neurocomputing 196:82–94
15. Dai J, Jia L, Xiao L (2021) Design and analysis of two prescribed-time and robust ZNN models with application to time-variant Stein matrix equation. IEEE Trans Neural Netw Learn Syst 32(4):1668–1677
16. Feng J, Qin S, Shi F, Zhao X (2018) A recurrent neural network with finite-time convergence for convex quadratic bilevel programming problems. Neural Comput Appl 30(11):3399–3408
17. Qiu B, Zhang Y, Yang Z (2018) New discrete-time ZNN models for least-squares solution of dynamic linear equation system with time-varying rank-deficient coefficient. IEEE Trans Neural Netw Learn Syst 29(11):5767–5776
18. Xiao L, Li K, Duan M (2019) Computing time-varying quadratic optimization with finite-time convergence and noise tolerance: a unified framework for zeroing neural network. IEEE Trans Neural Netw Learn Syst 30(11):3360–3369

19. Liu J, Zhang Y, Yu Y, Sun C (2020) Fixed-time leader–follower consensus of networked nonlinear systems via event/self-triggered control. IEEE Trans Neural Netw Learn Syst 31(11):5029–5037
20. Liu J, Zhang Y, Sun C, Yu Y (2019) Fixed-time consensus of multi-agent systems with input delay and uncertain disturbances via event-triggered control. Inf Sci 480:261–272
21. Zhang Y, Li S, Kadry S, Liao B (2019) Recurrent neural network for kinematic control of redundant manipulators with periodic input disturbance and physical constraints. IEEE Trans Cybern 49(12):4194–4205
22. Zhang Y, Li S, Zhou X (2019) Recurrent neural network based velocity-level redundancy resolution for manipulators subject to joint acceleration limit. IEEE Trans Ind Electron 66(5):3573–3582
23. Yu F, Liu L, Xiao L, Li K, Cai S (2019) A robust and fixed-time zeroing neural dynamics for computing time-variant nonlinear equation using a novel nonlinear activation function. Neurocomputing 350:108–116
24. Li W, Liao B, Xiao L, Lu R (2019) A recurrent neural network with predefined-time convergence and improved noise tolerance for dynamic matrix square root finding. Neurocomputing 337:262–273
25. Xu F, Li Z, Nie Z, Shao H, Guo D (2018) Zeroing neural network for solving time-varying linear equation and inequality systems. IEEE Trans Neural Netw Learn Syst 30(8):2346–2357
26. Li J, Zhang Y, Mao M (2019) General square-pattern discretization formulas via second-order derivative elimination for zeroing neural network illustrated by future optimization. IEEE Trans Neural Netw Learn Syst 30(3):891–901
27. Hu C, He H, Jiang H (2020) Fixed/preassigned-time synchronization of complex networks via improving fixed-time stability. IEEE Trans Cybern 51(6):2882–2892
28. Liang T, Zhang W, Dong J, Yang D (2023) Fixed/preassigned-time stochastic synchronization of T–S fuzzy complex networks with partial or complete information communication. ISA Trans 137:339–348
29. Qin X, Jiang H, Qiu J, Hu C (2023) Fixed/prescribed-time synchronization of quaternion-valued fuzzy BAM neural networks under aperiodic intermittent pinning control: a non-separation approach. Neuro. Comput 549:126460–126476
30. Hu C, Yu J, Chen Z, Jiang H, Huang T (2017) Fixed-time stability of dynamical systems and fixed-time synchronization of coupled discontinuous neural networks. Neural Netw 89:74–83
31. Ji G, Hu C, Yu J, Jiang H (2018) Finite-time and fixed-time synchronization of discontinuous complex networks: a unified control framework design. J Frankl Inst 355(11):4665–4685
32. Xiao L, Zhang Z, Li S (2019) Solving time-varying system of nonlinear equations by finite-time recurrent neural networks with application to motion tracking of robot manipulators. IEEE Trans Syst Man Cybern Syst 49(11):2210–2220
33. Luo J, Li K, Yang H, Yang J (2020) Comparison on inverse-free method and psuedoinverse method for fault-tolerant planning of redundant manipulator. IEEE Access 8:178796–178804
34. Xiao L, Tao J, Dai J, Wang Y, Jia L, He Y (2021) A parameter-changing and complex-valued zeroing neural-network for finding solution of time-varying complex linear matrix equations in finite time. IEEE Trans Ind Inform 17(10):6634–6643
35. Luo J, Yang H (2022) New variant-parameter ZNN solutions for resolving time-variant plural Lyapunov equation under preassigned time. IEEE Trans Ind Inform 19(5):6482–6491
36. Luo J, Yang H (2022) A robust zeroing neural network model activated by the special nonlinear function for solving time-variant linear system in predefined-time. Neural Process Lett 54(3):2201–2217
37. Zuo Z, Tie L (2014) A new class of finite-time nonlinear consensus protocols for multi-agent systems. Int J Control 87(2):363–370
38. Zuo Z, Tie L (2016) Distributed robust finite-time nonlinear consensus protocols for multi-agent systems. Int J Syst Sci 47(6):1366–1375
39. Tan Z, Li W, Xia L, Hu Y (2020) New varying-parameter ZNN models with finite-time convergence and noise suppression for time-varying matrix Moore–Penrose inversion. IEEE Trans Neural Netw Learn Syst 31(8):2980–2992
40. Xiao L, Dai J, Lu R, Li S, Li J, Wang S (2020) Design and comprehensive analysis of a noise-tolerant ZNN model with limited-time convergence for time-dependent nonlinear minimization. IEEE Trans Neural Netw Learn Syst 31(12):5339–5348